Journal of ETA Maritime Science 2023;11(2):119-126

Experimental Study of the Heave and Pitch Motions of an Inverted Bow Hull

Abolfath Askarian Khoob, Majid Askari Sayar, Karim Akbari Vakilabadi, Hassan Ghassemi

Marine Faculty of Imam Khomeini Maritime Academy, Nowshahr, Iran

Abstract

In this study, the experimental heave and pitch motion responses of inverted bow hulls in regular head waves were investigated. Comparison of the pitch and heave motion responses of two modified versions of an NA8-14 British Ship Research Association reference fishing vessel with 45 and 60 degrees inverted bows was performed. The findings showed that decreasing the inversion angle of the bow to 45 degrees improves the dynamic performance of the model. Moreover, the interactions between the heave and pitch motions led to the frequent appearance of "kinks" in coupled form in response to the heave and pitch motions.

Keywords: Inverted bow hull, Towing tank, Model test, Heave and pitch RAO, Seakeeping

1. Introduction

The lower amplitude of heave and pitch motions is favorable for the crews and passengers of ships. Also, the less displacement of ship cargo is another good result of calm and proper ship motion. In the past years, three different traditional ship bow forms, namely, vertical (e.g., Titanic ship bow form), Maier, and conventional, as well as unconventional bow forms such as axe bow, plump bow and inverted bow, have been used in ship design. The inverted or reversed bow design is of keen interest when designing ships [1-3]. It is a type of bow form that is used where reforming the hull to the back instead of ahead in the forepeak part of the ship (Figure 1) and is often accompanied by a negative tumblehome or flare over the ship hull length, for example, the US Navy destroyer Zumwalt 1000. However, the destroyer's seakeeping and dynamic performances are less known.

Gelling [4] studied the seakeeping performance of some realistic hull forms and revealed that the reverse bow increases the amplitude of pitch and heave motions but reduces vertical acceleration. An optimization procedure using different software tools has been developed by Boulougouris and Papanikolaou [5] and applied to investigate possible improvements of the hydrodynamic performance of the initial RO-PAX 2000 hull form with respect to total resistance and seakeeping. They revealed that application of an optimization procedure by genetic algorithms is very encouraging for the performances of very different bulbous bow shapes.

Akbari et al. [6] described the results of several seakeeping tests on a wave-piercing trimaran. They measured the heave and pitch motions at Froude numbers of 0.2, 0.37, and 0.51 and demonstrated that for lower Froude numbers, the interval between variations in the magnitudes of the RAOs of heave or pitch motions due to the change in the wavelength, wave frequency, and wave amplitude were not so wide. It has been revealed that regarding vertical motions and accelerations, ship resistance, water spray (deck wetness), slamming criteria, and signing, by using inverted bow form, many changes in ship responses can be expected. White et al. [7] investigated the resistance and seakeeping performance of the inverted bow form by a model test in a towing tank by constructing two models of the frigate FFG-7 using two 1:80 scale models in traditional form and another inverted bow form, revealing that the inverted bow reduces the resistance of the model and improves the seakeeping performance of the ships. Shahraki et al. [8] evaluated the effect of different

Address for Correspondence: Abolfath Askarian Khoob, Marine Faculty of Imam Khomeini Maritime Academy, Nowshahr, Iran
E-mail: askariankhoob@gmail.com
ORCID ID: orcid.org/0000-0001-8545-5837

Received: 11.06.2022
Last Revision Received: 25.12.2022
Accepted: 03.05.2023

To cite this article: A.A. Khoob, M.A. Sayar, K.A. Vakilabadi, and H. Ghassemi. "Experimental Study of the Heave and Pitch Motions of an Inverted Bow Hull." *Journal of ETA Maritime Science*, vol. 11(2), pp. 119-126, 2023.

bow forms on the motions of a segmented model, equipped with two 6 degrees of freedom force/torque sensors to measure dynamic loads. The results showed a significant variation in slam loads when comparing the three center bow lengths.

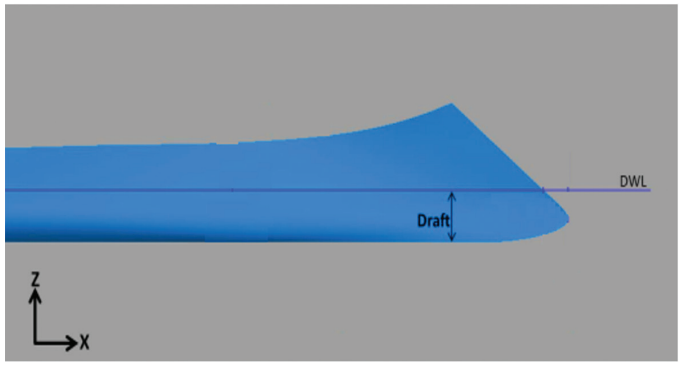

Figure 1. *Schema of ship with inverted bow shape*

Seo et al. [9] conducted model tests of a wave-piercing high-speed ship to examine the seakeeping performance at the towing tank. Their results demonstrated that vertical acceleration in the fore perpendicular region decreased by 11.3%. Mallat et al. [10] described the bubble sweep-down phenomenon on three bow designs by an experimental method and provided the performance of each bow geometry and the effect of bow shape changes in the face ON bubble sweep-down. Kim et al. [11] conducted model tests of a high-speed vessel with a modified inverted bow and showed an improved wave pattern by shifting the generation place of the forwarding divergent wave. Yuntao et al. [12] developed a multiobjective strategy to identify the parameters of pitch and heave coupled motions in ships to analyze the mathematical models for heave and pitch coupled and unknown parameters in dynamic equations.

Askarian Khoob et al. [13] conducted a series of model experiments using the National Iranian Marine Laboratory wave-piercing bow trimaran to determine the influence of outrigger symmetry on the heave and pitch motion responses. Nicolás et al. [14] selected the GNU SALOME platform as the working environment and developed a Python code to automate the shape construction of an inverted bow hull family from a series of input parameters. Shuling et al. [15] conducted a numerical comparative study using computational fluid dynamics on the seakeeping and added resistance of model ships with wave-piercing and "X-bow" monohulls in regular head waves.

In the literature, there are few technical data on the hydrodynamic performance of an inverted bow hull. Thus, this study investigates the effect of the inverted bow configuration on the dynamic performance of a reversed bow hull in regular head seas.

2. The Design of Two Experimental Models

The NA8-14 trawler of the British Ship Research Association was selected and scanned by a 3D scanner. The scanner output was imported into Rhino and SolidWorks to change it to an inverted bow with two different angles, namely, 45 and 60 degrees.

Figure 2 shows a plot of the 60 degree inverted bow form after changes in the software environment. Table 1 lists the main particulars of the prototype and its scaled models. Both models are 1/58th scale and do not have appendages. The vessel model was built with polylactic acid that has the capability of proper machining, superior resistance to water absorption, excellent impact-resistant performance, and smoothness surfaces for model construction. The midship and stern parts of the main hull were built without changes, but the forepart was changed to an inverted shape (Figure 2).

3. Experimental Testing Conditions

The objective was to assess the heave and pitch motion responses of the reverse bow design. Tests were performed at the towing tank of Nowshahr Maritime Academy, Iran. The test conditions and towing tank specifications are described. The load cell H3-C3-B3-D55 was procured from Zemek Company and can be carried up to 25 kg, and measure heave, pitch, yaw, roll, sway, and resistance data. The most important input for the test system is the speed of the model, which changes according to the type of test. The towing tank has a wavemaker maximum wavelength set at 4.85 m and towing carriage at 6 m/s maximum speed with dimensions 37 m × 3 m × 0.8 m. The model heave motion was measured using a potentiometer separately. Figure 3 shows the inverted bow model and towing tank load cell. The towing tank was outfitted with a flap and an electromechanical wavemaker with a frequency domain of 0.2 to 1.8 Hz. The water density was 1002 kg/m^3, and the temperature of the water was recorded at approximately 23 °C. With the connection of the arm to the model, at first,

Table 1. *Main particulars of the prototype and its scaled models*

Property	Ship	Model with 45° inverted bow	Model with 60° inverted bow
L_{pp}(m)	45.7	0.784 0.79	
T(m)	4.06	0.055-0.065	0.055-0.065
B(m)	8.03	0.138	0.138
$\nabla(m)^3$	839.5	0.004533	0.004538
C_w	0.775(-)		
C_b	0.564(-)		
C_p	0.627(-)		

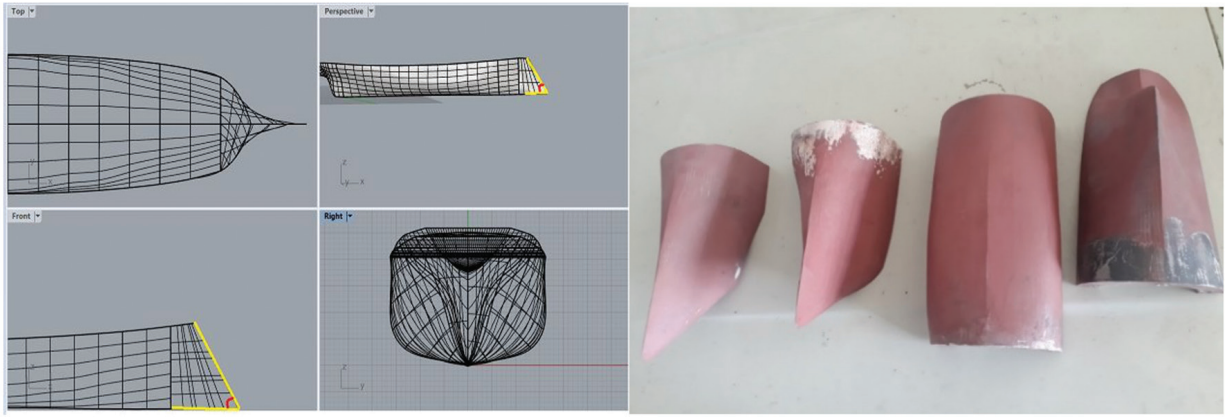

Figure 2. *Bow design and construction*

the center of gravity must be determined. Afterward, by placing the model in the towing tank, the amount of draft was checked so that it was consistent with the designed draft; then, the initial calibration was performed with great accuracy. With the wavemaker generating the proper wave, the model moves at a certain speed, and the load cell wirelessly sends the results to the computer. In Figure 3, the inverted bow model was configured into four separate parts: the aft and midship parts connected for overall tests were joined by nuts and bolts, but the fore segments in two inverted bow forms, 45 and 60 degrees, for any special test series were fixed.

Wave height H is directly related to the wavemaker stroke. Before testing the model, two parameters, namely, wavemaker stroke and frequency were entered into the wave maker to create regular waves. The calculation model velocity must be calculated according to the scale. Froude similarity can be written as;

$$\lambda = \frac{L_{ship}}{L_{model}} = 45/0.775 = 58 \quad (1)$$

$$(F_n)_{ship} = (F_n)_{model} \quad (2)$$

$$V_s/\sqrt{(L_s g)} = V_m/\sqrt{(L_m g)} \Rightarrow \quad V_s / V_m = \sqrt{(L_s/L_m)} = \sqrt{\lambda} \quad (3)$$

Assuming ship service speed to be 15 knots, the model speed can be expressed as;

$$V_{model} = V_{ship}/\sqrt{\lambda} = 15/\sqrt{58} = 1.976 \text{ knots} \quad (4)$$

$$V_{model} = (1.9760) \times (0.5144) = 1.013 \text{ m/s} \quad (5)$$

As a result, three speeds, namely, 0.6, 0.9, and 1.2 m/s, were considered for towing tank tests. The waves generated in the towing tank were of regular type, with wavelengths changing from 0.6 to 1.6 L by an increment of 0.2 L.

Two wave heights of 3 and 5 m, equal to the average wave height and the highest effective wave height of the Persian Gulf were considered for model testing. The scale wave height for the towing tank was obtained using Equation (6):

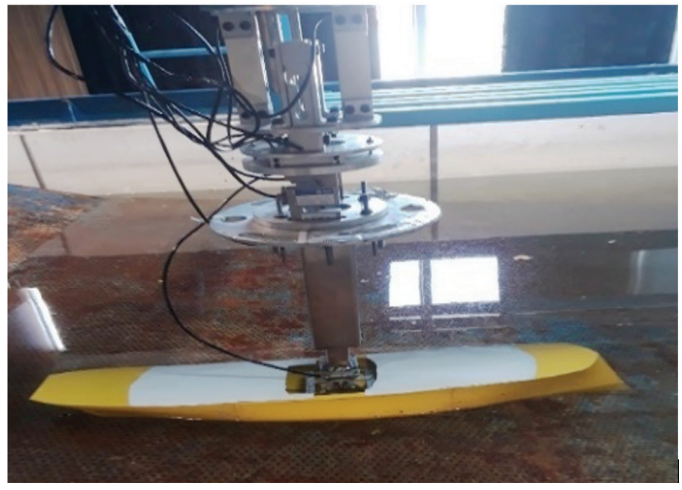

Figure 3. *The model with 60° inverted bow*

$$H_{model} = \frac{H}{\lambda} = \frac{3}{58} = 0.052m \quad (6)$$

$$H_{model} = \frac{H}{\lambda} = \frac{5}{58} = 0.086m \quad (7)$$

Thus, both values of the heave and pitch RAOs can be drawn against the encountering wave frequency (ωe) or the encountering wavelength (λ_w). To analyze the heave motion behavior in the model, a dimensionless property RAO (response amplitude operator) was calculated using

$$RAO_{Heave} = {}^{z_a}/_{\xi_a} \quad (8)$$

where heave z_a is the motion amplitude and ξ_a is the imposed wave amplitude for the model. The experimental model tests were performed at three speeds corresponding to ship speeds from 0.6 to 1.2 m/s at 0.3 increments. To avoid the occurrence and subsequent spurious measurement of results in the presence of any reflected waves and residual decaying, a waiting period between the respective tests of 20-40 min (depending on the wave amplitude and frequency) was allowed. Water surface was also visually controlled.

4. Experimental Testing Conditions

In this study, there were 36 runs of individual tests per model comprising six wave frequencies, two wave heights, and three vessel speeds performed on each of the two models.

4.1. Heave Motion

Figures 4-6 illustrate the comparison of the heave motion responses of the two models, revealing non-linear responses concerning the wave frequencies as well as plots containing the "kink." The "kink" is due to the coupling of the heave and pitch motion responses at their respective frequencies. These changes in vessel speeds affect the peak magnitude response of the models. Some of these kinks are the resonance effects on the model. The responses for the 60 degree inverted bow contain kinks with higher magnitude than those for the 45 degree inverted bow. The comparison of the heave motion responses for the two models shows significantly different trends, but their magnitudes increase with increasing model speed. There is a clear distinction between their magnitudes (Figures 4a and 6b): the 60 degree inverted bow model has higher magnitudes at the same vessel speeds, wave height, and all frequencies than the 45 degree inverted bow model. In Figures 4a and 6b, the 45 degree inverted concept performs better than the 60 degree one in terms of having lower magnitudes of motion responses. In other words, low inversion angles for the bow hull suggest proper seakeeping effects compared with high angles of the inverted bow. In Figure 5b, at a speed test of 0.9 m/s, the heave RAOs for the 60 degree inverted bow model are less at lower frequencies. Figure 6a shows a harmonic behavior of heave RAO for both 45° and 60° inverted bow in various λ_w/L. It is observed that at λ_w/L, 0.9 - 1.3 the 45 degrees inverted concept performs better than the 60 degrees inverted bow in this research.

A comparison of the heave motions concerning the three model speeds for two different wave heights shows that the responses at speed 0.9 m/s correspond to the vessel cruise speeds: the 60 degree inverted bow model has the highest responses at higher non-dimensional wavelengths. At 1.2 λ_w /L, a rise can also be identified for more plots of heave RAO. It is found that the model speed of 1.2 m/s experiences a significant high RAO for the 45 and 60 degree inverted bows. In addition, these curves show a peak region of the heave RAO. These changes may identify the resonance region. Again, in higher λ_w/L heave, RAO experiences a descending characteristic. At 1.2 m/s speed, the model experiences the highest responses at all non-dimensional wavelengths. At 0.052 m wave height, the responses are visibly high compared with the wave height of 0.086 m wave height, which has a lower response.

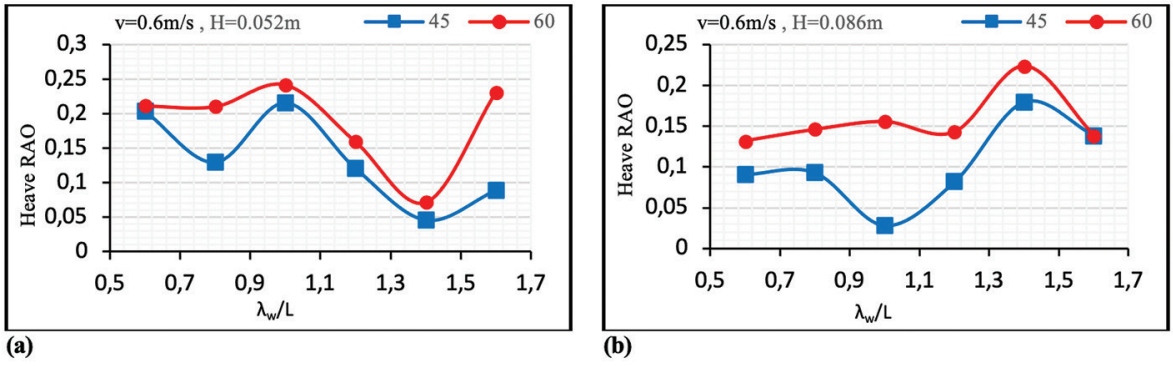

Figure 4. *Comparison of heave RAOs at v=0.6 m/s, (a): H=0.052 m and (b): H=0.086 m*

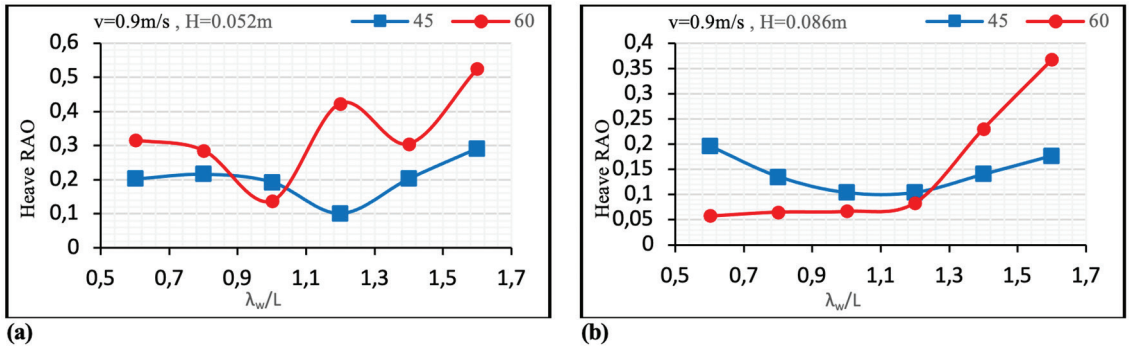

Figure 5. *Comparison of heave RAOs at v=0.9 m/s, (a): H=0.052 m and (b): H=0.086 m*

4.2. Pitch Motion

Figures 7-9 exhibit a comparison of the pitch motion responses of the two models. As observed, the responses contain "kinks" (as described above) that are more visible in the 60 degree inverted bow plots. The responses for the 60 degree inverted bow contain kinks with higher magnitude than those for the 45 degree inverted bow. Comparison of pitch motion responses for the two models shows that their trends are significantly different, but the 60 degree inverted bow model has higher magnitudes at the same vessel speeds, wave height, and most frequencies than the 45 degree inverted bow model. Each graph shows the change in pitch RAOs due to wave and speed changes. Similar to the heave motion in the pitch motion response comparisons, it has been established that the 45 degree inverted configuration performs better than the 60 degree one in terms of having lower magnitudes of pitch motion responses. Figure 8b shows the maximum pitch RAO of the 45 degree inverted bow model at 1.4 λ_w/L. It is observed that loss occurred suddenly. As predicted, Figure 9b demonstrates a larger pitch RAO for the 1.2 m/s speed; as seen in λ_w/L 1.0 to 1.6, there is a high rise of pitch RAO of the 60 degree inverted bow configuration. However, outside this two-pitch region, RAO is nearly identical.

A comparison of the heave motions concerning the model speeds at two different wave heights shows the responses at a speed of 0.9 m/s and a wave height of 0.0522 m (which corresponds to the vessel cruise and top speeds): the 60 degrees inverted bow model has the highest responses at higher non-dimensional wavelengths. The model

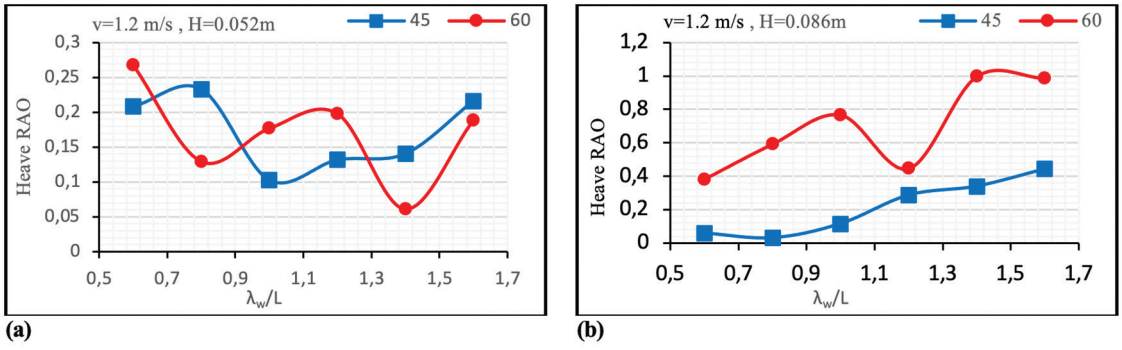

Figure 6. *Comparison of heave RAOs at v=1.2 m/s, (a): H=0.052 m and (b):H=0.086 m*

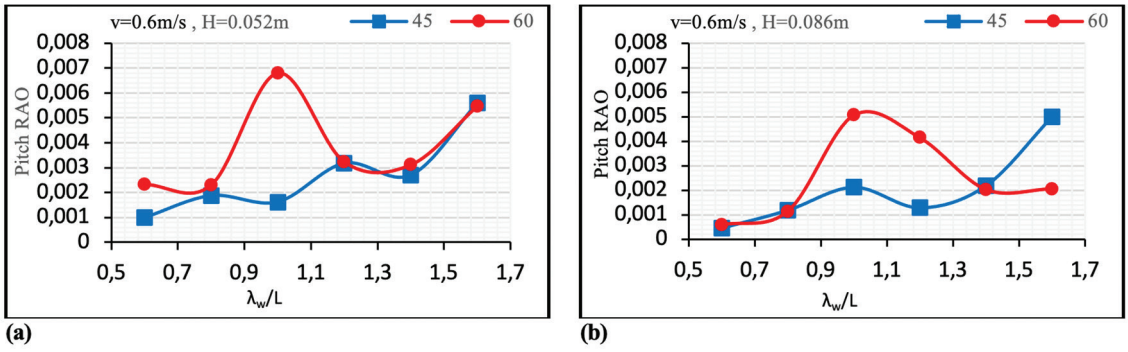

Figure 7. *Comparison of pitch RAOs at v=0.6 m/s, (a): H=0.052 m and (b): H=0.086 m*

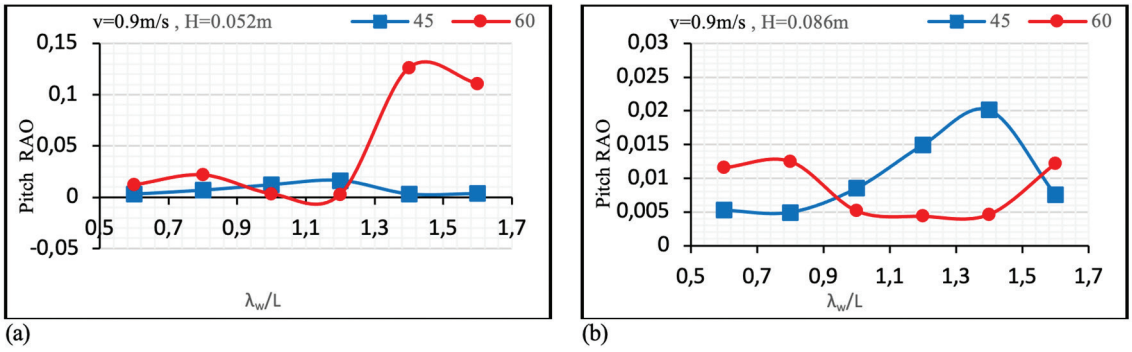

Figure 8. *Comparison of pitch RAOs at v=0.9 m/s, (a): H=0.052 m and (b): H=0.086 m*

experienced the highest magnitudes at a wave height of 0.086 m, and the responses were visibly higher than those at a wave height of 0.052 m, that have a lower response. It should be mentioned that by changing the value of λ_w/L from 0.6 to 1.6, a slight change occurs in the pitch RAO except for the case of model speed 1.2 for the 60 degree inverted bow.

Figure 10 illustrates the design of the conventional bow form in the software to compare with the results of the behavior of the inverted bow form, revealing that the RAO values are different from the conventional ship RAO values,

Figure 11 illustrates the harmonic behavior of heave RAO for the conventional bow form model and 60 degree inverted bow in various λ_w/L (at v=0.6 m/s).

A table of changes (Table 2) was obtained to compare the values of the inverted bow form with the conventional bow form.

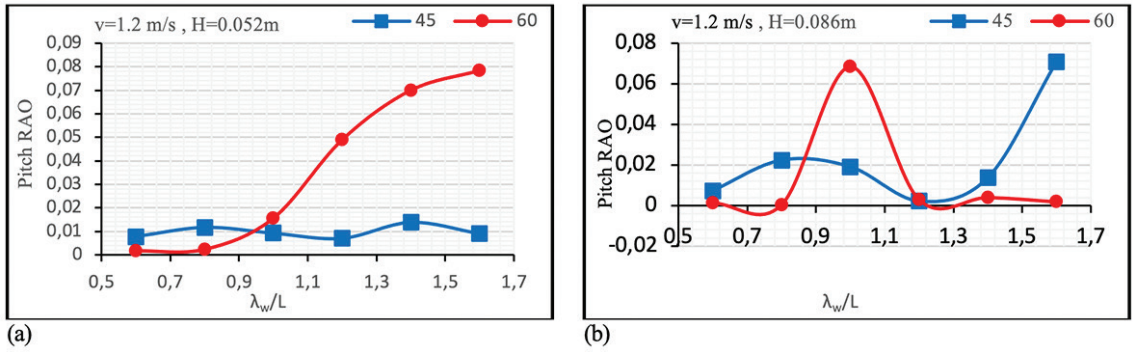

Figure 9. *Comparison of pitch RAOs at v=1.2 m/s, (a): H=0.052m and (b): H=0.086 m*

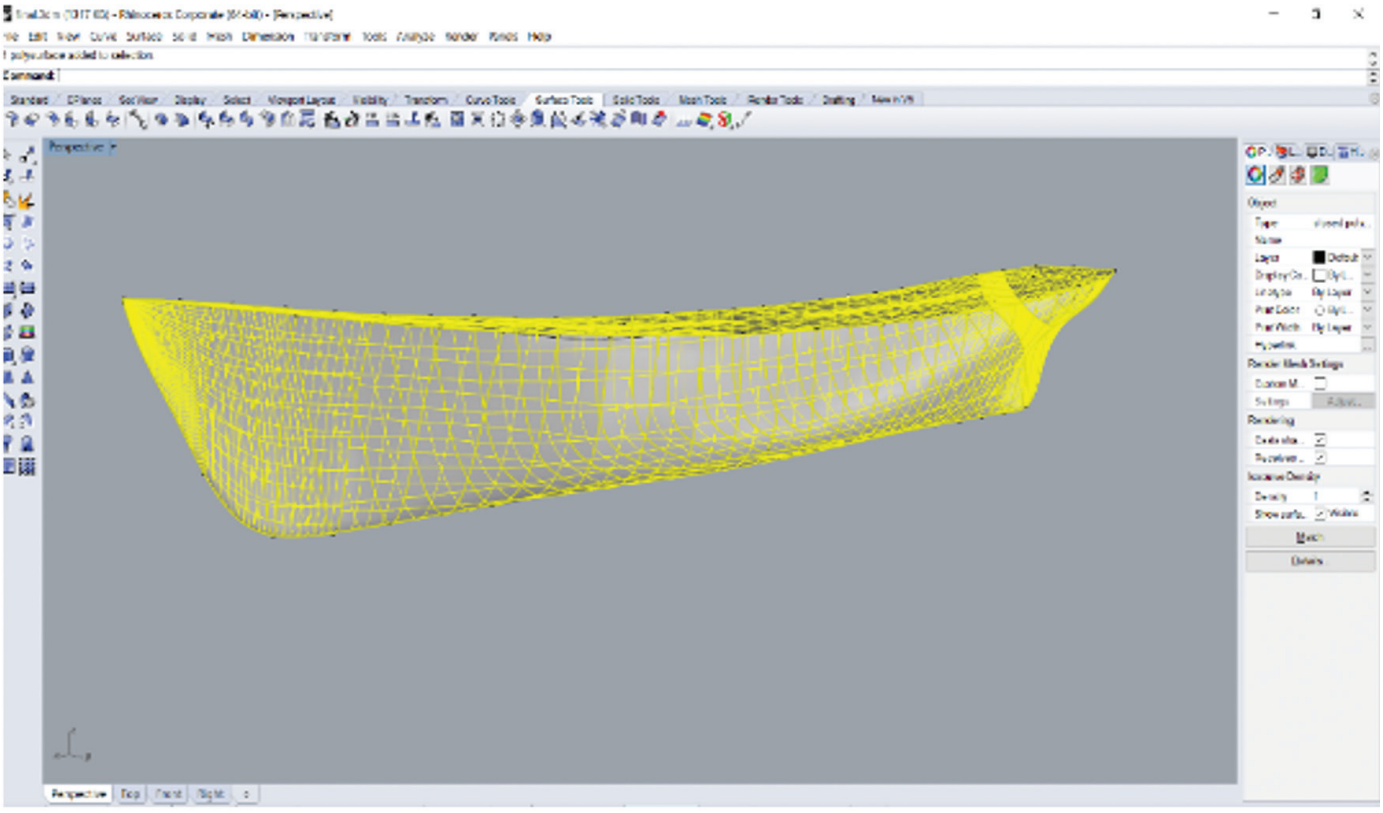

Figure 10. *Designed conventional bow form in the software*

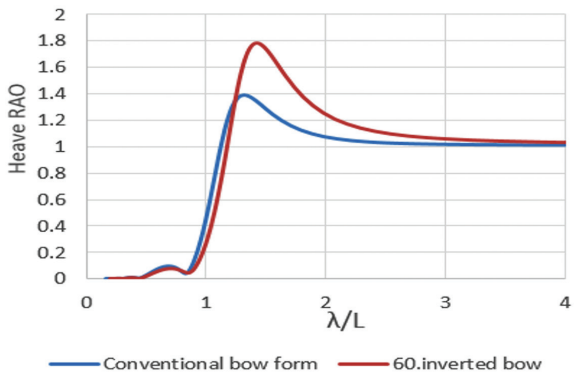

Figure 11. *Heave RAO for conventional bow form model and 60° inverted bow in various λ_w/L (at v=0.6 m/s)*

Table 2. *The average changes in the RAO movement of inverted bow form with conventional bow form*

Test speed	The average change in percentage of heave's movement ratio	
	From the beginning point until the maximum point of Rao heave (for conventional bow form)	From the maximum point of heave Rao for conventional bow until the end of the range
$u_1 = 0/6\frac{m}{s}$	-28.12%	17.7%
$u_2 = 0/9\frac{m}{s}$	-47.1%	21.2%
Overall average percentage change	37.47%	20.2%
The negative percentage of heave RAO, shows smaller amounts for inverted bow shape*		

5. Conclusion

A series of seakeeping tests to measure the heave and pitch motions of an inverted bow hull with two inversion angles, 45 and 60 degrees, were performed at the towing tank of Nowshahr Maritime Academy.

It was found that the 45 degree inverted bow (shorter inverted bow) offered better performance in waves than the 60 degree configuration. The reason for this behavior is more cutting water waves to the sides, which were observed in most experimental tests related to the 45 degree inverted bow model compared with the 60 degree inverted bow model.

The interactions between the heave and pitch motion responses led to the frequent appearance of "kinks" in the coupled form. These couplings were observed mostly at higher frequencies and hurt performance of the vessel. Such "kinks" were also attributed to the effects of vessel speed changes because their magnitudes usually increase when the vessel speed increases.

The responses for the 60 degree inverted bow contained kinks with higher magnitude than those for the 45 degree inverted bow. The comparison of the heave motion response for the two models showed significantly different trends, but their magnitudes increased with increasing model speed.

Peer-review: Externally peer-reviewed.

Authorship Contributions

Concept design: Data Collection or Processing: Analysis or Interpretation: Literature Review: Writing, Reviewing and Editing: All authors have contributed equally.

Funding: The author(s) received no financial support for the research, authorship, and/or publication of this article

References

[1] A. Kükner, and K. Sanöz, "High speed hull form optimization for seakeeping," *Advances in Engineering Software,* vol. 22, pp. 179-189, 1995.

[2] A. Maimun, O. Yaakob, A. Kamal, and N. Chee, "Seakeeping analysis of a fishing vessel operating in Malaysian water," *Jurnal Mekanikal,* vol. 22, pp. 103-114, Dec 2006.

[3] J. A. Keuning, G. L. Visch, J. L. Gelling, W. Vries, and G. Burema, "Development of a new SAR Boat for the Royal Netherlands sea rescue institution," *Proceedings of the eleventh International Conference on Fast Sea Transportation,* Hawaii, USA, 2011, pp. 797-806.

[4] J. L. Gelling, "The axe bow: the shape of ships to come," *Proceedings of the ninth in 19th International Symposium on Yacht Design and Yacht Construction,* Amsterdam, Netherlands, 2006.

[5] E. Boulougouris, and E. A. Papanikolaou, "Hull form optimization of a high-speed wave piercing monohull," *Proceedings of the ninth International Marine Design Conference,* Ann Arbor-Michigan, 2006.

[6] K. Akbari Vakilabadi, M. R. Khedmati and M. S. Seif, "Study on heave and pitch motion characteristics of a wave-piercing trimaran," *Transactions of FAMENA,* vol. 38, pp. 13-26, Jan 2014.

[7] J. K. White, S. Brizzolara, and W. Beaver, "Effect of inverted bow on the hydrodynamic performance of navy combatant hull form," *SNAME Transactions,* vol. 123, pp. 2-16, Nov 2015.

[8] J. R. Shahraki, G. Thomas, I. Penesis, and W. Amin, "Centrebow design for wave-piercing catamrans," *Proceedings of the 12th International Conference on Fast Sea Transportation,* Amsterdam-Netherland, 2015.

[9] J. Seo, et al. "Model tests on resistance and seakeeping performance of wave-piercing high-speed vessel with spray rails," *International Journal of Naval Architecture and Ocean Engineering,* vol. 8, pp. 442-455, Sep 2016.

[10] B. Mallat, G. Germain, B. Gaurier, P. Druault and J. Y. Billard, "Experimental study of the bubble sweep-down phenomenon on three bow," *Journal of Ocean Engineering,* vol. 148, pp. 361-375, Jan 2018.

[11] D. J. Kim, N. Hyun and K. Jung, "A study on the effect of hull appendages of high-speed catamarans with modified-reverse

bow on the running performance," *Journal of the Korean Society of Marine Environment & Safety,* vol. 25, pp. 601-608, 2019.

[12] D. Yuntao, C. Ran and Y. Xin, and L. Liqiang, "Hydrodynamic coefficients identification of pitch and heave using multi-objective evolutionary algorithm," *Ocean Engineering,* vol. 171, pp. 33-48, Jan 2019.

[13] A. Askarian Khoob, S. Moghaddam Puor, and A. Feizi, "Experimental investigation of a Wave-Piercing Trimaran on the outrigger configurations in terms of seakeeping and added resistance," *Journal of Applied Fluid Mechanics*, vol. 15, pp. 51-62, Feb 2022.

[14] A. A. Nicolás, et al. "A parametric share modeler tool for inverted bow fishing vessel." Mecánica Computacional, vol XXXVIII, pp. 413-423, 2021.

[15] C. Shuling, Z. Beilei, H. Changzhi, and Y. Shiqiang, "Comparative study on added resistance and seakeeping performance of X-bow and wave-piercing monohull in regular head waves," *Journal of Marine Science and Engineering,* vol. 10, pp. 813, June 2022.